REPORT DOCUMENTATION PAGE

AFRL-SR-AR-TR-04-

0198

Public reporting burden for this collection of information is estimated to average 1 hour per response, including the time for reviewing instruction data needed, and completing and reviewing this collection of information. Send comments regarding this burden estimate or any other aspect c this burden to Department of Defense, Washington Headquarters Services, Directorate for Information Operations and Reports (0704-0188), 12 4302. Respondents should be aware that notwithstanding any other provision of law, no person shall be subject to any penalty for failing to com valid OMB control number. PLEASE DO NOT RETURN YOUR FORM TO THE ABOVE ADDRESS.

1. REPORT DATE (DD-MM-YYYY)	2. REPORT TYPE	3. DATES COVERED (From - To)
03-25-2004	Final	12-15-2000 to 6-30-2003

4. TITLE AND SUBTITLE
Lightweight, High-Strength, Age-Hardenable Nanoscale Materials

5a. CONTRACT NUMBER

5b. GRANT NUMBER
F49620-01-1-0127

5c. PROGRAM ELEMENT NUMBER

6. AUTHOR(S)
Vijay K. Vasudevan and Jainagesh A. Sekhar

5d. PROJECT NUMBER

5e. TASK NUMBER

5f. WORK UNIT NUMBER

7. PERFORMING ORGANIZATION NAME(S) AND ADDRESS(ES)

University of Cincinnati
Department of Chemical and
Materials Engineering, 401B
Rhodes, PO Box 210012,
Cincinnati, OH 45221-0012

8. PERFORMING ORGANIZATION REPORT NUMBER

9. SPONSORING / MONITORING AGENCY NAME(S) AND ADDRESS(ES)
AFOSR/NA
Metallic Structural Materials
4015 Wilson Blvd., Room 703
Arlington, VA 22203-1954
Monitor: Dr. Craig S. Hartley

10. SPONSOR/MONITOR'S ACRONYM(S)

11. SPONSOR/MONITOR'S REPORT NUMBER(S)

12. DISTRIBUTION / AVAILABILITY STATEMENT

Public/Unclassified/Unlimited

DISTRIBUTION STATEMENT A
Approved for Public Release
Distribution Unlimited

13. SUPPLEMENTARY NOTES

14. ABSTRACT
Phase transformations and precipitation behavior in age-hardenable nanoscale materials, using binary aluminum alloys as model materials, were studied. Nanoparticles of Al-Cu and Al-Zn were synthesized by a plasma ablation process. The particles (50-100nm dia) were found to be supersaturated f.c.c. and were enveloped by a 2-4 nm amorphous Al oxide layer. On aging the Al-Cu nanoparticles, a precipitation sequence comprising nearly pure Cu precipitates to θ′ to the equilibrium θ was observed, with all three forming along the Al oxide-matrix interface. In the Al-Zn nanoparticles, a spinodal structure was noted in the as-synthesized state, which evolved into a striated, f.c.c. twinned platelet structure within which were contained hcp precipitates also in twin relation; nearly pure Zn precipitates also formed along the Al oxide-matrix interface. Ultra fine Al-Cu nanoparticles were also synthesized by inert gas condensation; these were found to be quite stable against precipitation during aging. Finally, the results revealed that Al nanopowders could be processed into bulk structures, leading to interesting Al-Al oxide nanocomposites with full densification and high hardness.

15. SUBJECT TERMS

16. SECURITY CLASSIFICATION OF:			17. LIMITATION OF ABSTRACT	18. NUMBER OF PAGES	19a. NAME OF RESPONSIBLE PERSON
a. REPORT	b. ABSTRACT	c. THIS PAGE	None	27	Vijay K. Vasudevan
Unclassified	Unclassified	Unclassified			19b. TELEPHONE NUMBER (include area code) (513) 556-3103

20040423 030

Best Available Copy

LIGHTWEIGHT, HIGH-STRENGTH, AGE-HARDENABLE NANOSCALE MATERIALS

Final Report

Work Performed Under

Grant No.: F49620-01-1-0127

Period: 12/15/00 to 6/30/03

Submitted By

Vijay K. Vasudevan and Jainagesh A. Sekhar

Department of Chemical and Materials Engineering,
University of Cincinnati, Cincinnati, Ohio 45221-0012
Phone: (513)-556-3103; Fax: (513)-556-3773;
E-mail: vijay.vasudevan@uc.edu; jainagesh.sekhar@uc.edu

To

Dr. Craig S. Hartley
Program Manager, Metallic Structural Materials
Air Force Office of Scientific Research/NA, 4015 Wilson Blvd., Room 703
Arlington, VA. 22203-1954

March 25, 2004

TABLE OF CONTENTS

1. Executive Summary

In the current project, phase transformations and precipitation behavior in age-hardenable nanoscale materials systems, using binary aluminum alloys as model materials, were studied. A major objective was to establish a basic understanding of the evolution of structural changes within individual nanoparticles of these alloys, as well as of the structural and physical characteristics of consolidated bulk pieces produced therefrom.

Nanoparticles of bulk Al-4.4 wt.% Cu and Al-15 wt.% Zn were synthesized by rapid plasma ablation followed by rapid quenching and the aging behavior of these particles was studied using x-ray diffraction, conventional and high-resolution transmission electron microscopy and nanoprobe energy dispersive x-ray analysis. The particles were found to be in the supersaturated f.c.c. state in both cases, but displayed a variation in the individual particle composition (0.5 to 4.5 wt.% Cu, 15-40 wt.% Zn) when compared with the precursor bulk alloys. All the particles were found to contain a 2-5 nm thick adherent aluminum oxide scale, which prevented further oxidation. On aging the Al-Cu nanoparticles, a precipitation sequence consisting of, nearly pure Cu precipitates to the metastable θ' to equilibrium θ–Al_2Cu was observed, with all three forming along the oxide-particle interface. The structure of θ' and its interface with the Al matrix has been characterized in detail. In the Al-Zn alloy, a spinodal structure was noted in the as-synthesized particles. The spinodal structure coarsened on aging into an f.c.c. twinned platelet structure that contains h.c.p. precipitates also in twin relation. Nearly pure Zn precipitates, with an h.c.p. structure, also formed along the oxide-particle interface and consumed the spinodal structure with time. Ultra fine Al-Cu nanoparticles (5-25 nm dia) were synthesized by inert gas condensation (IGC) and their aging behavior was studied. These particles were found to be quite stable against precipitation.

Finally, the sintering and consolidation behavior of aluminum nanoparticles were studied. It was found that nanopowders of Al could be processed via thermal and thermo mechanical means to bulk structures with high hardness and density. Temperature and time of sintering were found to have a dominant effect. The sintering process led to breakup of the oxide scale, leading to an interesting nanocomposite composed of 100-200 nm Al oxide dispersed in a bimodal nanometer-micrometer size Al matrix grains, which retained high hardness. Cold rolling and hot rolling were effective methods for attaining full densification and high hardness.

2. INTRODUCTION AND OBJECTIVES

Nanoscale materials have the potential to enable the significant leaps required in the science, technology and application of new lightweight, high-strength, high conductivity, medium-temperature materials in ever-demanding energy, transportation, propulsion, space, and structural systems. Although there has been considerable research on nanoscale materials in recent years and discoveries made of new phenomena and novel properties, such as enhanced strength compared with their bulk counterparts [1-13], the behavior of nanoscale alloys and related materials that are compositionally metastable and hence vulnerable to solid-state phase changes during thermal or other treatments, is, however, far from being known, both within the individual "nano" building blocks, as well as in bulk consolidated forms composed of these nanoentities.

In the current project, we have focused on binary aluminum alloys as model materials for the study of phase transformations and precipitation behavior in age-hardenable nanoscale materials systems [14-17]. A major objective was to establish the science-based understanding of the evolution of structure and chemistry of the fundamental nanoscale particles, the interfaces between them, as well as of the structural and physical characteristics of the consolidated bulk pieces. In particular, we investigated basic science issues related to the precipitation behavior when the supersaturated parent phase grain or particle size approaches the same nanoscale (1-100nm) dimensions as critical nuclei and transition phases like GP zones. The issue of whether spinodal decomposition can occur at these "nano" length scales, along with effects of variation in the grain or particle size on this process, was also studied. Binary age-hardenable Al-Cu and Al-Zn alloys that allow us to probe the effects of lattice mismatch and spinodal decomposition on the precipitation behavior was the primary focus of the work. In addition, Inert Gas Condensation (IGC) was used to synthesize ultra fine nanoparticles of Al-Cu and the aging behavior of these particles was studied. Lastly, the processing of nanoscale powders of aluminum to bulk structures was investigated.

3. ACCOMPLISHMENTS

The accomplishments of the present project are covered in three parts, as described below

3.1. Synthesis of Al-Cu and Al-Zn Nanoparticles and Their Aging Behavior

Synthesis of Nanoparticles and Characterization Methods

Ingots of two alloy compositions were initially made, namely, Al-4.4 wt%Cu alloy and Al-15 wt%Zn. As discussed below, the compositions of the particles were found to be modified (after converting to the nanocrystalline state) when compared with the original bulk compositions. Ultra high purity (5-9's) raw materials (~300g) were melted under clean nitrogen PlasmaAirtorch* atmosphere in a graphite crucible. The alloys were cast into 2" dia. x 2" long ingots. The Al-Cu ingots were solution heat treated at 545°C for 50 hrs, whereas the Al-Zn ingots were solution heat-treated at 450°C for 50 hrs. The ingots were next sent for making the nanoparticles.♣ Although conditions under which the particles were made were proprietary, the following details could be surmised. The process for the synthesis of nanoparticles relies upon a "plasma gun" for creating an arc between two electrodes, to produce a metal vapor plasma, which is rapidly quenched to form a gas phase suspension of nanoscale metal particles (Figure 1). The power discharge typically is 30–100 MW per shot and .the nanoparticles produced are collected in the ESP. The company normally manufactures oxide and other non-metallic powders, typically 10- 50nm diameter in size. The mean particle size from BET measurements and the corresponding amount of material is given in Table 1 below for the Al alloy nanoparticles synthesized for this study.

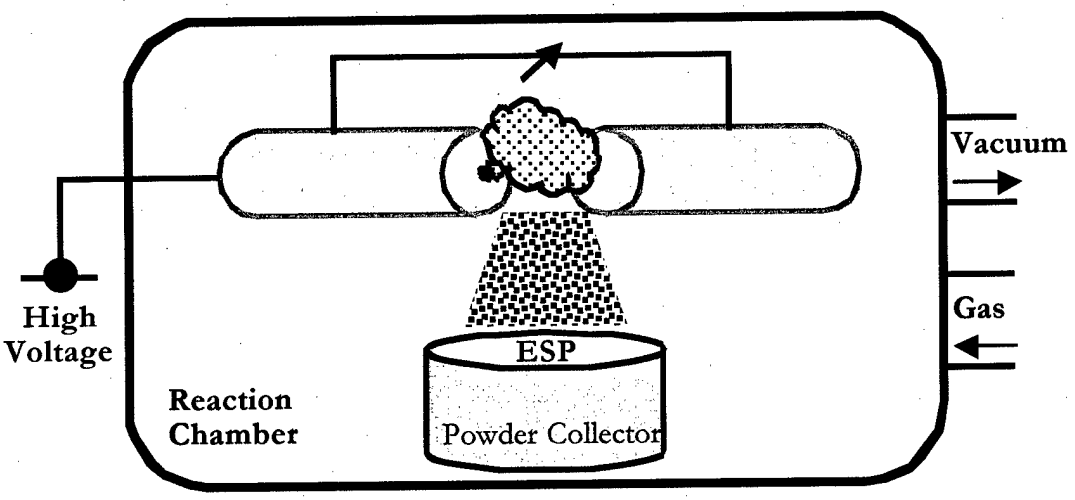

Figure 1—Schematic of plasmas ablation process for the synthesis of nanoparticles (from Nanotechnologiers, Inc., Austin, TX).

* The PlasmaAirtorch is a trade mark of MHI Inc. Cincinnati, OH 45208
♣ The particles were made by Nanotechnologies, Inc., Austin, TX 78758

The particles were examined in the as-received (called as-synthesized in the rest of the text) condition and in the aged condition. Aging was conducted by heating the particles in evacuated and Argon back filled capsules, which also had a thin titanium strip placed in them that was heated with a oxyhydrogen torch to getter oxygen. For the Al-Cu particles, aging was conducted at 130°C and 190°C for times ranging from 1 to 10 h. The Al-Zn were aged at 65, 130 and 190°C, again for durations ranging from 1 to 10h.

Table 1. The typical collection of nano particles per run.

Average Particle Size, nm	Collection in the ESP per run, mg
136	656
130	587
86	80
92	482

The nanoparticles were characterized by x-ray diffraction, SEM, TEM and energy dispersive x-ray spectroscopy (EDS) in the TEM. Prior to TEM observations, the nanoparticles were dispersed in methanol in an ultrasonic unit and then deposited onto carbon-coated nickel grids using a pipette. TEM observations were performed using a Philips CM20/CM200 (LaB_6 and FEG sources) microscope operated at 200kV under bright field (BF) dark field (DF) conditions and selected area diffraction (SAD) modes; the HRTEM observations were performed using a JEOL-4000EX operated at 400kV and JEM-1000 ARM operated at 1MeV. For determining the chemical compositions of the particles, x-ray spectra were recorded using ultra-thin window EDS systems fitted to the TEM; standardless analysis was used to ascertain particle/phase compositions.

Microstructure of As-synthesized Nanoparticles

The as-synthesized Al-Cu and Al-Zn alloy particles were single-phase f.c.c with a lattice parameter of ~0.404nm, ranged in size from 20-150nm (average of ~90 nm) and faceted along {111} planes (Fig. 2(a,b)). Occasionally, particles with diameters greater than 200 nm wee noted. An adherent oxide scale 2-4 nm in thickness was enveloped the particles, as revealed by HRTEM (Figs. 2(c,d)). This oxide was amorphous. EDS analysis revealed considerable variation in the amount of Cu (from 0.5 to 4.5 wt% Cu) and amount of Zn (from 24-62 wt.% Zn), in the Al-Cu and Al-Zn particles, respectively. Typical EDS spectra are shown in Figure 3. Although the Al-Zn particles were all single phase (supersaturated), the microstructure was noted to be mottled inside the particles (indicative of spinodal decomposition), with the mottling becoming more apparent in higher Zn concentrations particles. Occasionally, pure Zn particles were also noted. No dislocations were seen in any of the particles.

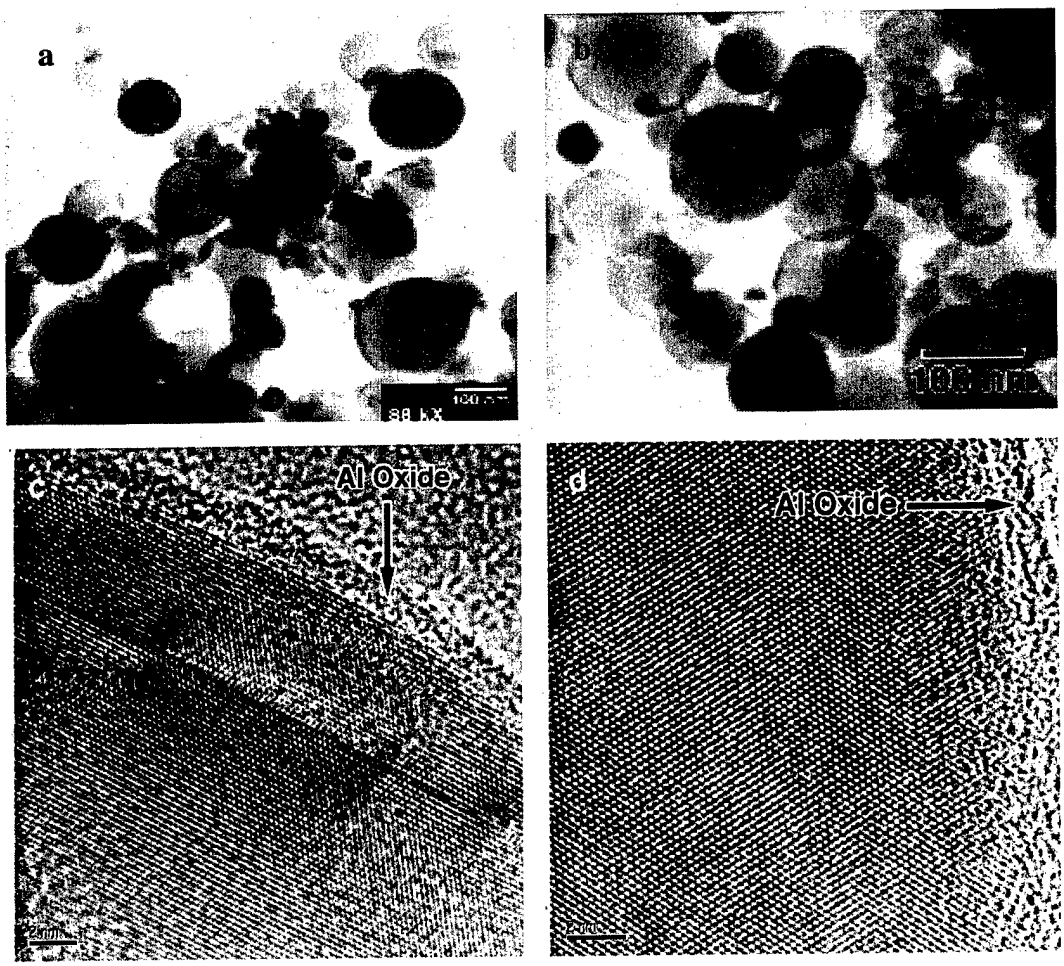

Figure 2—BFTEM (a,b) and HRTEM (c,d) micrographs of as-synthesized nanoparticles of (a,c) Al-Cu and (b,d) Al-Zn. Note defects due to radiation damage in (c).

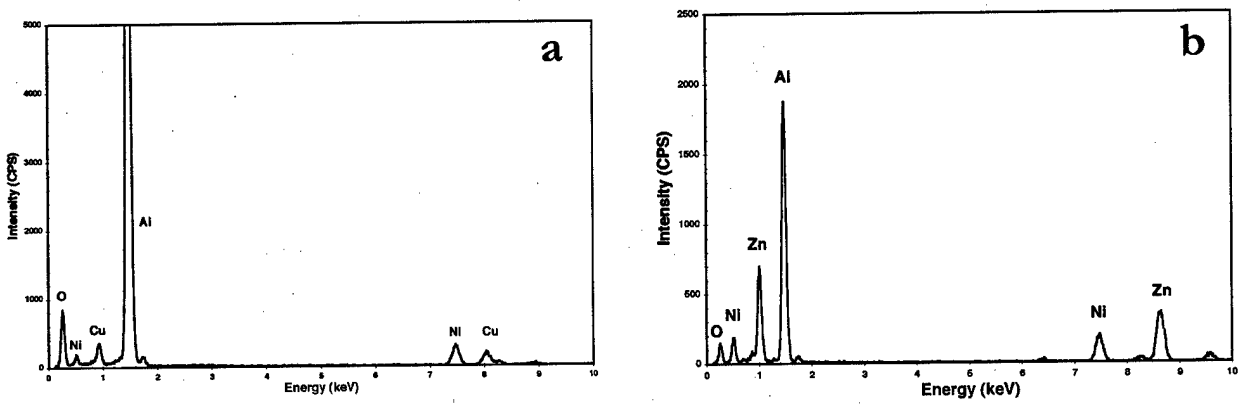

Figure 3—Typical EDS spectra recorded from as-synthesized (a) Al-Cu and (b) Al-Zn nanoparticles. Note: Ni peaks come from the supporting grid.

Aging Behavior of Al-Cu Nanoparticles

Upon aging at 130 and 190°C, plate-shaped precipitates, with length of about 20-40nm and thickness of about 5-20 nm, appeared within 1h (Figure 4). Analysis of EDS spectra indicated that many of the precipitates were highly enriched in Cu (80-95 wt.%), whereas others had lower Cu, between 35-55 wt.%, near that of Al_2Cu (the composition of equilibrium θ and of the metastable θ'). The beam size of the electron probe was about 2-5nm, so some sampling from the adjacent regions may be expected. In all cases, the precipitates formed at the aluminum oxide/particle interface. Aging for longer times led to the appearance of larger number of precipitates within the particles (Fig. 2(b)) and the compositions of most of these were between 35-55 wt.% Cu, i.e. near that of Al_2Cu. The particle matrix was largely depleted of Cu, containing about 0.2-0.4 wt.%. At short times, the precipitate-matrix interface appeared quite sharp/straight (and apparently coherent), but became curved at longer times, presumably due to loss of coherency.

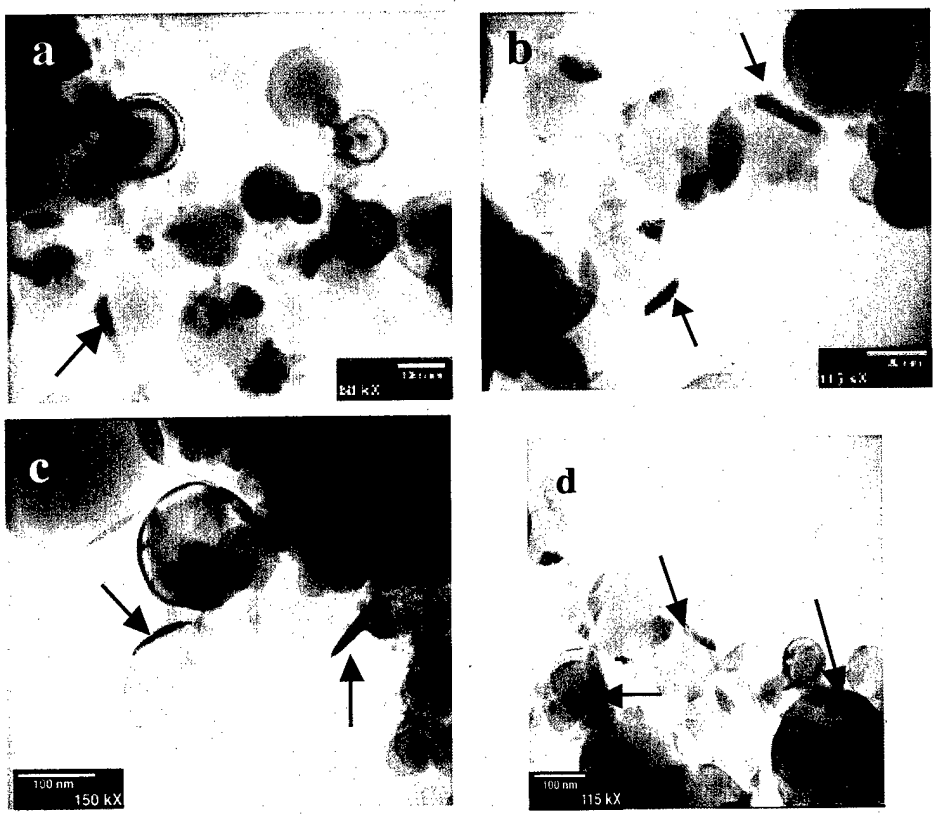

Figure 4—BF images of Al-Cu nanoparticles aged at 130°C for (a) 1h and (b) 10h and at 190°C for (c) 1h and (d) 10h. Note the appearance of the second phase precipitates within the particles (indicated by arrows) along the oxide-particle matrix interface.

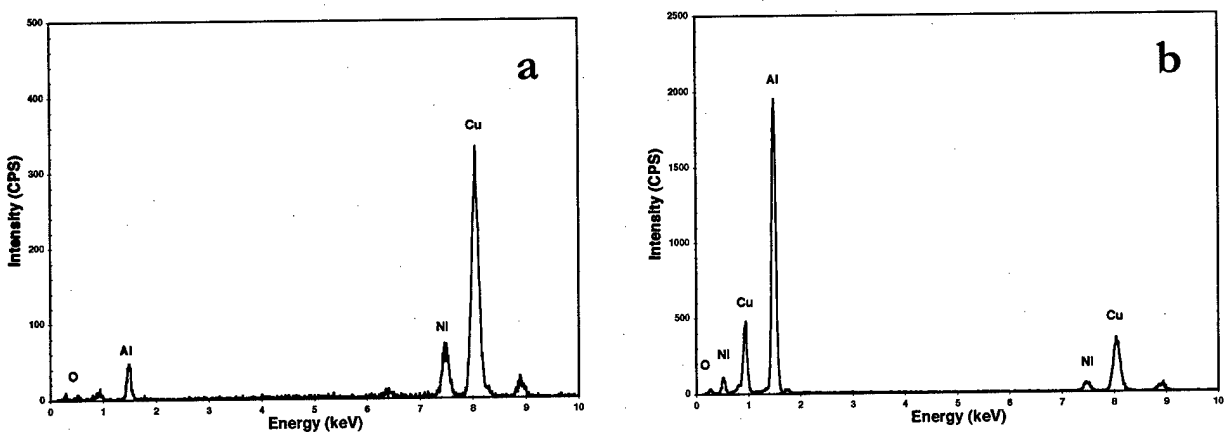

Figure 5—Typical EDS spectra recorded from aged Al-Cu nanoparticles. (a) Cu-rich precipitates and (b) precipitates with composition near Al_2Cu. Note: Ni peaks come from the supporting grid.

The highly Cu-rich precipitates appeared to be GP zones, though their structure has not been determined yet. However, it was noteworthy and the thickness of these is over an order of magnitude greater than those of GP zones in conventional, coarse-grained materials. Many of the precipitates with compositions near Al_2Cu were determined to be θ'. [010] and [110] CBED patterns recorded with a very fine probe from regions including these precipitates and the matrix are shown in Figs. 6(a) and

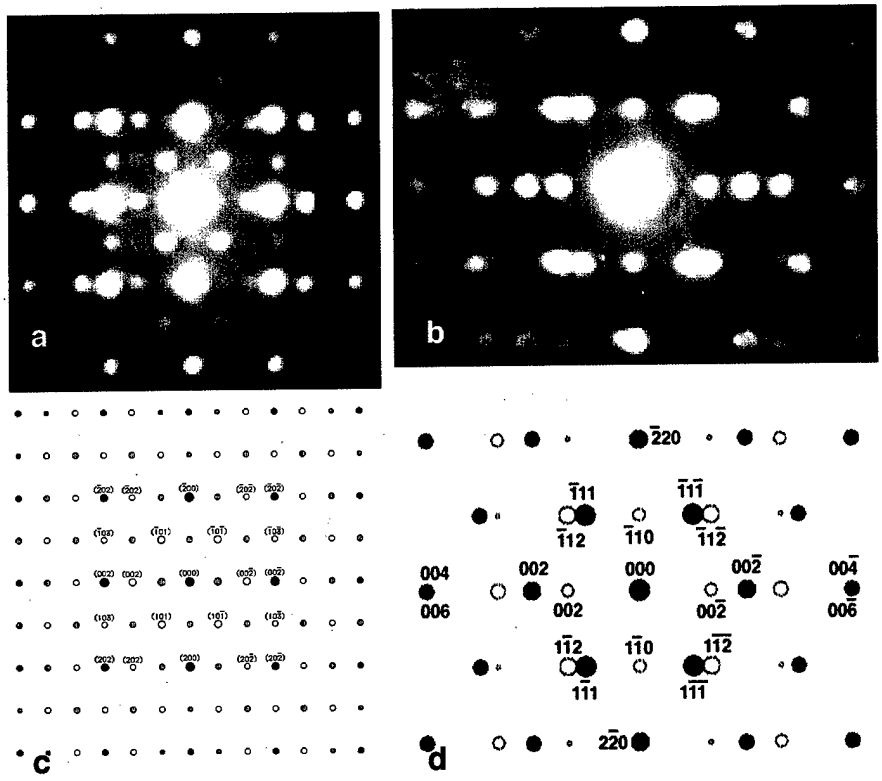

Figure 6—CBED patterns (a) [010] Al/θ' and (b) [110] Al/θ' and computer-simulated diffraction patterns (c) [010] and (d) [110] identifying the θ' precipitate in particles aged at 190°C, 1h; in (c,d) the solid circles denote matrix reflections, the open circles θ' reflections and shaded circles double diffraction reflections.

6(b), respectively. By means of computer simulations, Figs. 6(c) and 6(d), the patterns could be indexed on the basis of a body centered tetragonal structure with lattice parameters **a**=4.04 Å and **c**=6.075 Å and orientation relationship of (001) Al // (001) θ' and [010] Al // [010] θ'. It should be noted that the **c**-parameter determined differed slightly from the value of 5.8Å reported for θ' in bulk, coarse-grained aged Al-Cu alloys [18], whereas the **a**-parameter was the same. As a result the (006) reflection of θ' nearly coincides with the (004) of Al and the mismatch with the matrix along the **c**-axes is reduced. In bulk Al-Cu, the θ' is fully coherent along the broad faces (i.e. (001) plane), but semi-coherent along the edges [18].

An HRTEM micrograph recorded along the [110] beam direction, Fig. 7(a), shows the structure of the θ', the matrix and the interface between them. The interface consists of terraces parallel to the (002) plane interspersed with ledges ~1-2 (002) planes tall at which extra half planes corresponding to dislocations are present, i.e. the broad faces are coherent, but the edges are semi-coherent. When viewed along the [010] direction, Fig. 7(b), the θ' and α-Al matrix appear perfectly coherent across the (002) interface plane, along with perfect matching of the (200) planes. While the interface is for the most part straight, long and sharp, atomic scale

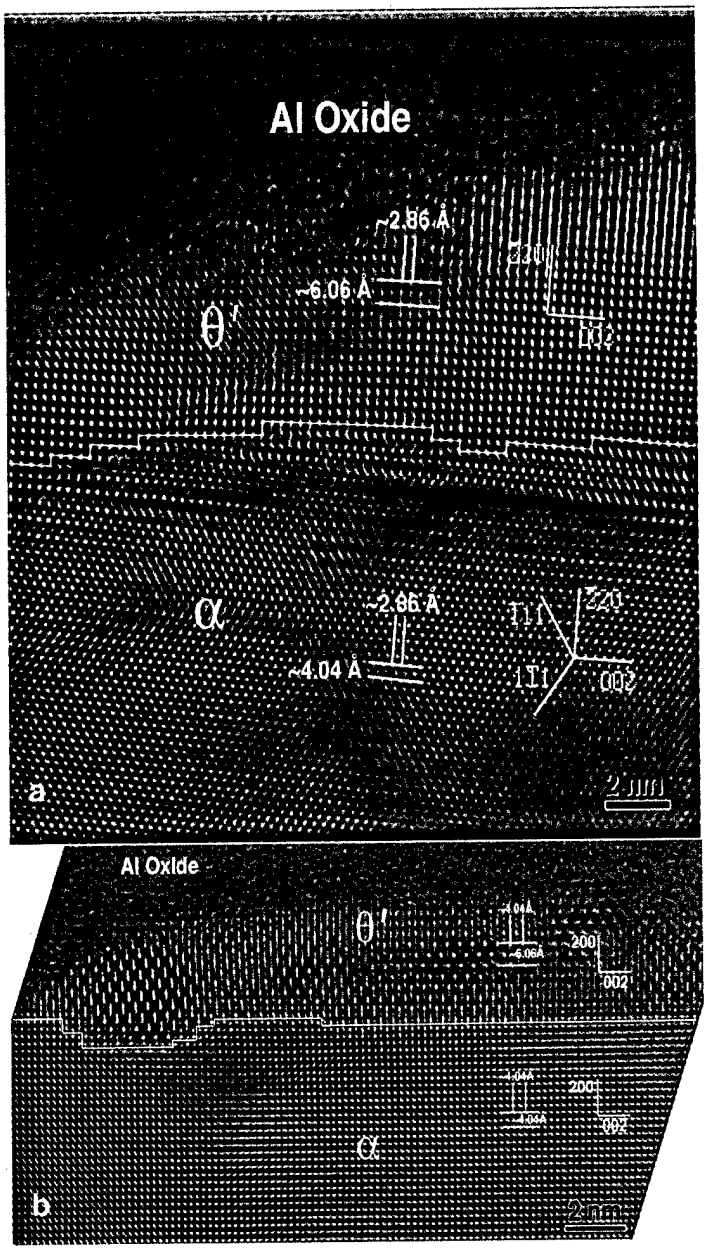

Figure 7—HRTEM micrographs recorded along the (a) [110] Al/θ' (aged at 190°C, 1h) and (b) [010] Al/θ (aged at 130°C, 1h) showing the structure of the α-Al matrix, the θ' precipitate and interface between them in a nanoparticle.

facets with steps or ledges 1-2 (002) planes tall between facets can be seen in some parts. In this case, the θ' spans across the peripheral length of the parent matrix particle, with the edges contacting the outer Al oxide. The misfit dislocations expected along the edges (parallel to the (200) plane) to accommodate the mismatch in the [001] direction are not seen and presumably the amorphous Al oxide accommodates the entire mismatch. In addition to θ', some of the precipitates were determined to be the equilibrium θ-Al_2Cu phase (Fig. 8). Misfit dislocations could be seen along the precipitate-matrix interface.

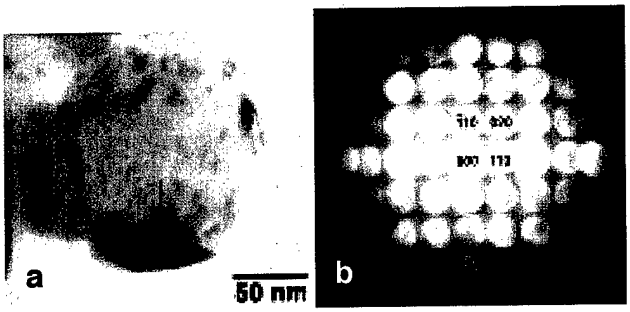

Figure 8—(a) BF micrograph and (b) [001] CBED pattern identifying the equilibrium θ-Al_2Cu precipitate (arrowed) in Al-Cu nanoparticles aged at 190°C, 1h.

Aging Behavior of Al-Zn Nanoparticles

The Al-Zn alloy showed mottled structures, especially in the higher Zn particles even in the as-synthesized condition (Fig. 2(b)). Figs. 9(a,b) show the wide variation in microstructures observed for this alloy following aging for 1h. Most of the particles displayed two types of features: (a) a striated structure in two orientations, and (b) a much coarser precipitate that formed along the oxide/particle surface. Analysis of EDS spectra (Fig. 10 (a) indicated that the latter were nearly pure Zn (85-95wt%), and diffraction analysis indicated that the structure was h.c.p. (Fig. 9(c)). No low-index OR could be ascertained for these h.c.p. Zn-rich precipitates with the matrix, suggesting they are incoherent. EDS analysis indicated that the striations consisted of high and low zinc rich regions, but the structure was f.c.c with some evidence for splitting of reflections along the <111> directions (Fig. 9(d)). Analysis of EDS spectra (Fig. 10(b)) of regions including the striations and the surrounding matrix gave a typical composition of 35-45 wt% Zn. The striated structure evolved into a structure composed of platelets in f.c.c. twin relationship, within which were contained precipitates also in twin relationship (Fig. 11(a)). This morphology gave rise to complex diffraction effects (Fig. 11(b)). Analysis suggested that the precipitates within the f.c.c twin-related regions have an h.c.p. structure. At long times, the platelet structure yielded to the pure Zn precipitates, whose number increased over that observed after shorter time aging.

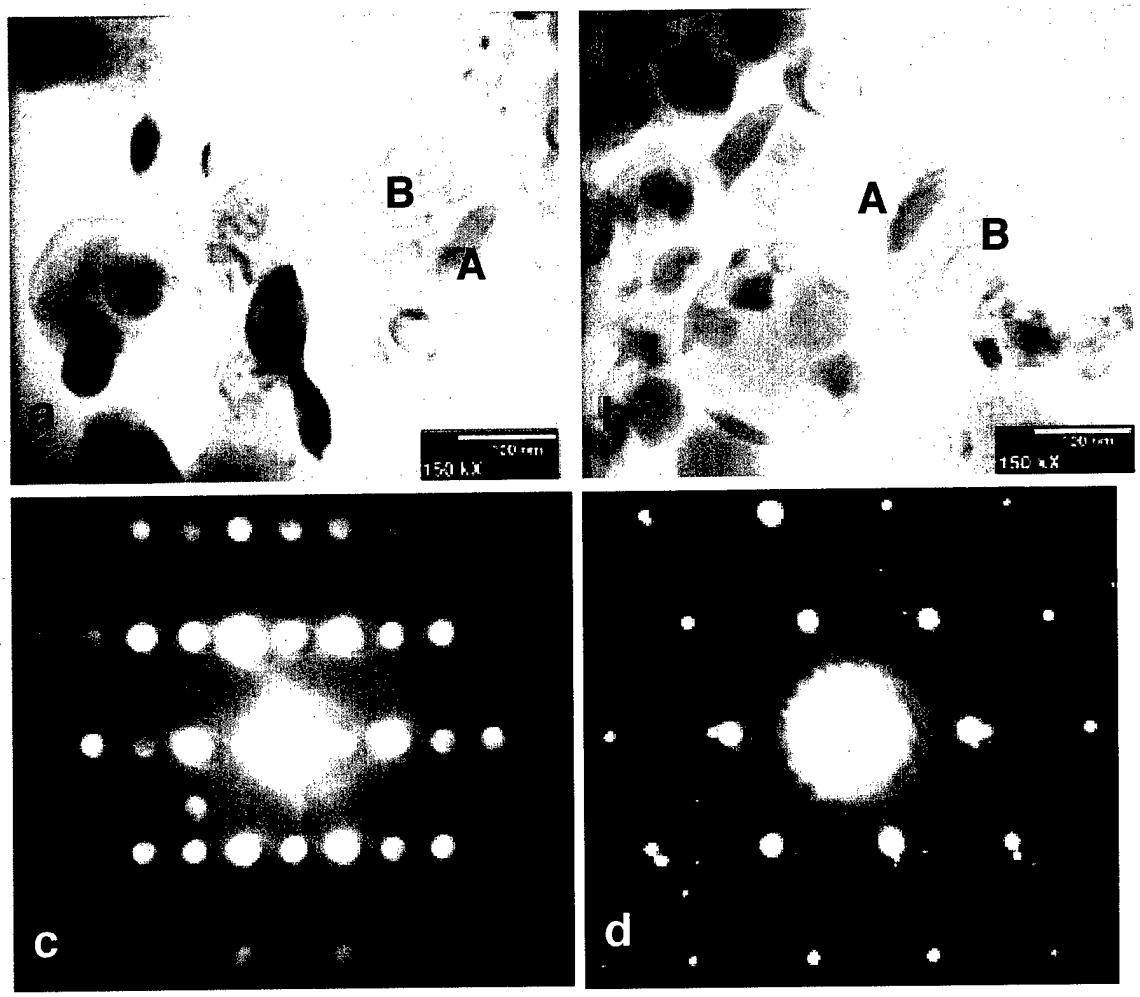

Figure 9—Al-Zn particles aged at 130°C. (a) 1h, BF image; (b) 10h, BF image; (c) [11-20] CBED pattern establishing the hcp structure of the Zn-rich precipitates, and (d) [011] SAD pattern from striated structure within the particles. Note the two types features in the particles, viz., Zn-rich precipitates labeled A and the striated (spinodal) structure labeled B and splitting of reflections along <111> in (d) from this structure.

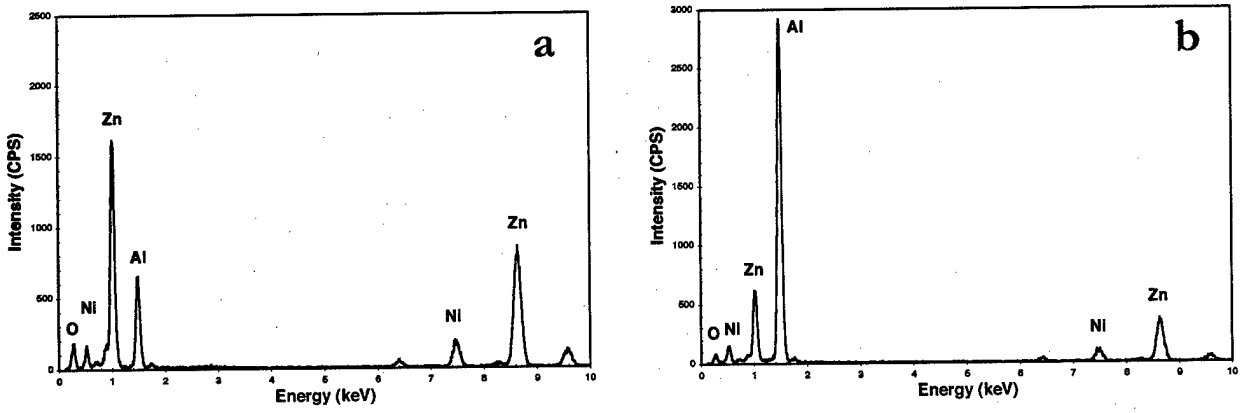

Figure 10—Typical EDS spectra recorded from aged Al-Zn nanoparticles. (a) Zn-rich precipitates and (b) striated structure + matrix. Note: Ni peaks come from the supporting grid.

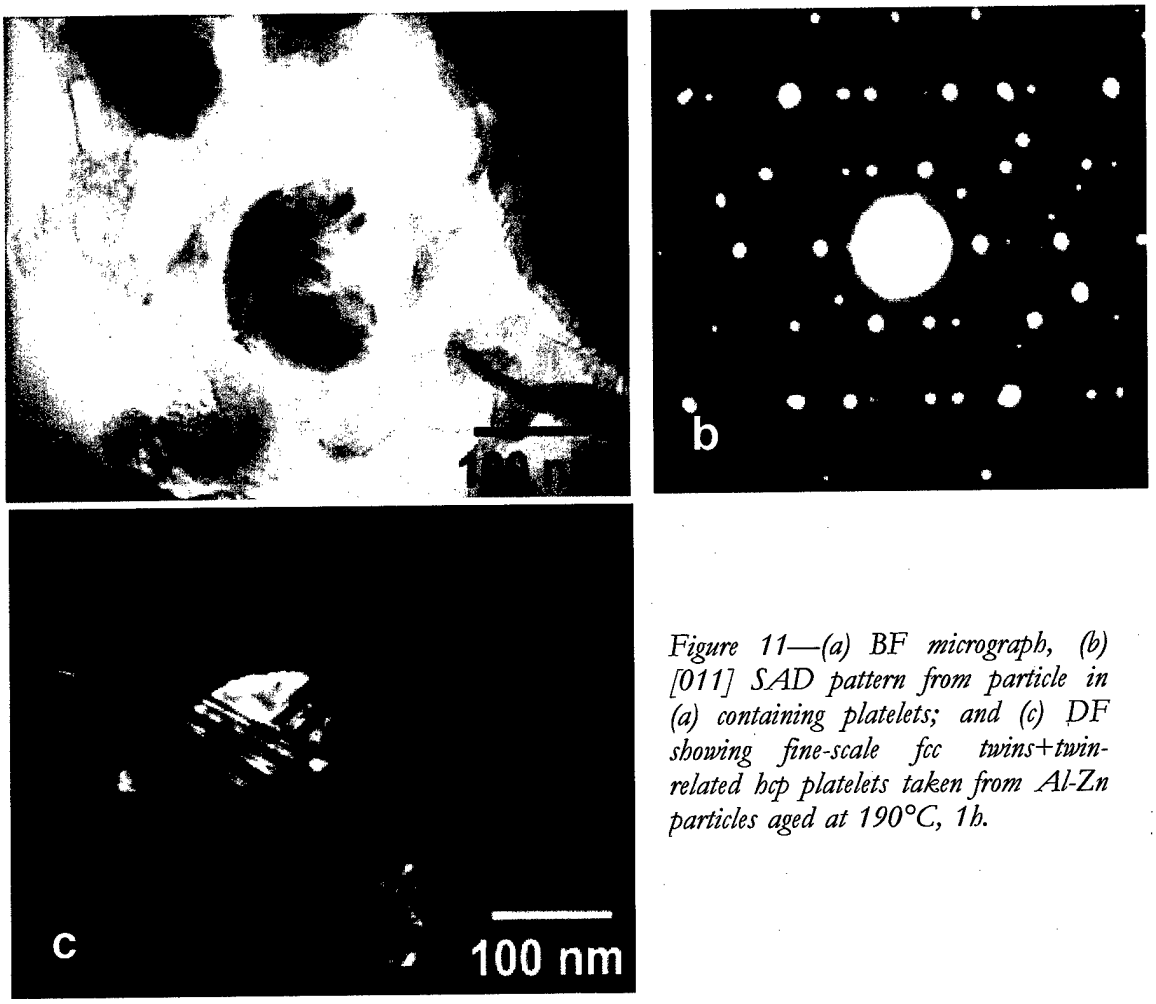

Figure 11—(a) BF micrograph, (b) [011] SAD pattern from particle in (a) containing platelets; and (c) DF showing fine-scale fcc twins+twin-related hcp platelets taken from Al-Zn particles aged at 190°C, 1h.

Discussion

The as-synthesized nanoparticles of the alloys were single phase and except for some mottling noted in the Al-Zn alloy particles no other features such as dislocations or grain boundaries were observed. All particles were coated with a 2-4 nm thick amorphous aluminum oxide layer. After the heat treatment, a common feature noted in both alloys was that the precipitation appeared to initiate at the aluminum oxide/particle interface. Normally only one precipitate per particle was noted after aging.

On aging, the supersaturated Al-Cu nanoparticles appeared to follow a decomposition sequence normally noted in bulk alloys [18,19], although some clear differences were noted. In

bulk alloys, the precipitation at 130°C (generally inferred from hardness measurements) begins in 1 hr and reaches a peak at 100 hrs with a plateau region in the 10 hr range. During this process, initially the GP zones nucleate on defects such as dislocations or collapsed vacancy clusters and then further possibly coarsen to θ", while metastable Al-Cu regions (called θ') also begin to appear. The GP zones and θ" display coherency with the matrix and are associated with some lattice strain. At the 100h time exposure, the volume fraction of such precipitates is high [19,20]. The GP zones are about 1-3nm in thickness and 10 nm in diameter. The distance between individual GP zones in bulk alloys is about 2-4nm and about 10^{14} –10^{15} zones are formed per mm^3, i.e. a cube with a 10nm edge, would be expected to contain roughly one GP zone. The distance between the θ" precipitates is larger, being ~20-100nm. Eventually at very long times or higher temperatures, the equilibrium Al_2Cu precipitates appear, which are incoherent with the matrix. The appearance of the GP zones is associated with an increase in the hardness of the alloy; peak hardness is normally seen when θ' appears; the equilibrium phase is normally associated with a drop in hardness of the alloy.

In the Al-Cu nanoparticles, the sequence of precipitation was inferred to be: supersaturated solid solution to very high Cu concentration precipitates to θ' precipitates to precipitates with compositions and structure corresponding to the equilibrium θ-Al_2Cu. For the nanoparticles aged at 130°C and 190°C for 1 hr, the plate-shaped Cu-rich regions were noted to form in thicknesses much larger than conventional GP zones (10-20nm vs.1-3nm). Generally, only one precipitate per particle was noted and these appeared with a straight, sharp interface and coherent with the Cu depleted matrix. The θ'-matrix interface consisted of terraces parallel to the (002) plane interspersed with ledges ~1-2 (002) planes tall at which extra half planes corresponding to dislocations are present, i.e. the broad faces are coherent, but the edges are semi-coherent, as in the case of coarse-grained aged materials. On the other hand, the degree of misfit between the θ' and the Al matrix along the [001] direction appeared to be lower in the nanoparticle case compared with the situation in bulk, coarse-grained aged alloys and there was evidence that this misfit was partially accommodated by the outer amorphous aluminum oxide layer in contact with these precipitates. These observations are unusual compared with alloys in bulk form when similar heat treatments are carried out; as mentioned earlier, the θ' precipitates are always seen with a ring of surrounding dislocations. Once the precipitation began in the particles, the matrix was quickly depleted in Cu (within 1 hr) and remained so during subsequent aging.

In the Al-Zn alloy case, one key observation was that the nanoparticles were significantly enhanced in zinc content when compared with the parent ingot. It appears that the Zn may have vaporized in larger quantities during the ablation process and when the particles were cooled, the excess zinc was trapped in the nanoparticles. A spinodal-like microstructure was observed within the as-synthesized nanoparticles. For compositions greater than 30-wt%Zn, spinodal decomposition is expected from thermodynamic considerations [21,22]. Again, differences in the rate of formation and decay of the spinodal were observed in the nanoparticles when compared with bulk alloys. The spinodal structure evolved during aging into a striated composed of Al-rich and Zn-rich regions with an f.c.c. structure and parallel to {111} planes. Splitting of reflections in the SAD patterns along the <111>-f.c.c directions suggests that the initial composition fluctuations also develop along these directions. The mottled/spinodal structure in the as-synthesized particles displayed an average wavelength of about 7nm, and the treatment at 130°C (1-10 hrs) showed striated structures with wavelengths in the 10-20nm range. As the zinc content of the particles varied considerably when compared with the bulk ingot, it was difficult to compare these results with those inferred from early stage spinodal theory [22]. Occasionally, the striated structure appeared in the form of thin platelets in f.c.c. twin relationship within which were contained platelets with an h.c.p. structure also in twin relationship. Apart from these features, zinc-rich (85-95 wt% Zn) precipitates, apparently incoherent, also formed during aging at the aluminum oxide/particle interface and eventually replaced the striated spinodal structure. It should be noted that in bulk Al-Zn alloys with high Zn, spinodal decomposition occurs rapidly and the modulated, spinodal structure is replaced by a product composed of alternate Al-rich and Zn-rich plates originating from a cellular reaction that commences at the grain boundaries. A paper based on these various results is about to be submitted to *Acta Materialia* [15].

3.2. Synthesis and Aging Behavior of Ultra-Fine Nanoparticles of Al-Cu

It is clear from the preceding that the nanoparticles produced by the plasma ablation process were generally large, with an average size of ~90 nm, a size much larger than the typical dimensions of GP zones or other transition phases. Thus, in order to study the precipitation behavior when the length scales of the primary particle approached those of GP zones, the IGC facility at Argonne National Lab was used to synthesize ultra fine nanoparticles of Al-Cu. Several experiments were

performed to establish the optimum conditions, namely, evaporation temperature, chamber pressure, evaporation time and chamber venting, for synthesizing the nanoparticles of Al-Cu. Since ultra fine Al nanoparticles are susceptible spontaneous oxidation and conflagration, considerable care had to be exercised while admitting air into the chamber after the nanoparticles had been scraped from the cold finger and collected. Venting the chamber to atmosphere had to be done extremely slowly (over several hours) to form only an outer layer of oxide around the particles and prevent subsequent/complete oxidation.

TEM analysis of material made by vaporizing an Al-4Cu charge revealed that Al nanoparticles 5-25 nm in diameter were produced, but very little Cu was present in the particles. This was not surprising, since the vapor pressure of Al is nearly ten times that of Cu near the melting temperature of Cu. Consequently, in subsequent experiments, pure Cu was added to the Al-4Cu charge to bring the overall composition to ~30 wt.%Cu, melted and vaporized together and the nanoparticles collected. TEM analysis revealed that Al-Cu alloy nanoparticles (5-25 nm dia), with 3-7 wt.% Cu resulted (Fig. 12); in addition, ~8 wt.%Si was also present in the particles (the latter may have come from the alumina/mullite crucible used to melt the charge in the IGC). It is interesting to note, however, that the particles still had a single-phase f.c.c structure

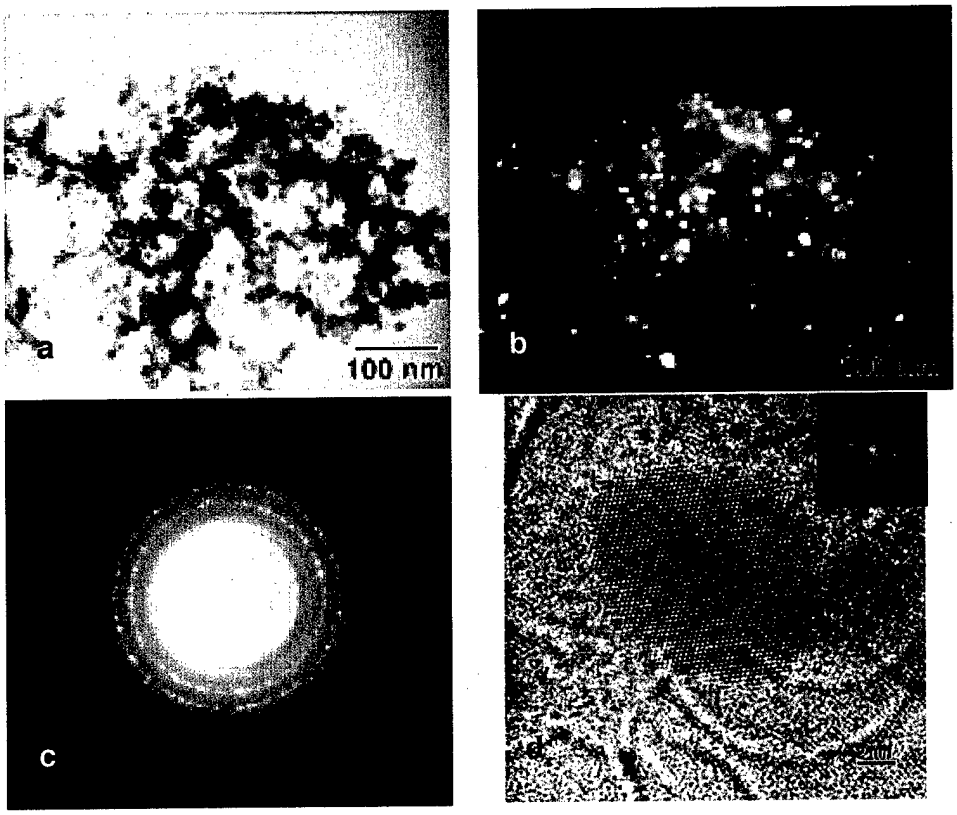

Figure 12–(a) BF micrograph, (b) DF micrograph from (111) Al reflection and (c) SAD pattern and (d) HRTEM along [011] fcc (inset FFT) from Al-Cu nanoparticles synthesized by IGC using Al-4Cu + pure Cu (overall Al-30 wt.% Cu) charge.

with lattice parameter near that of Al and supersaturated in Cu and Si. The particles were encapsulated in quartz under Argon and aged at 190°C and 300°C. Observations of the aged particles by conventional TEM (Fig. 13) revealed that other than some particle coarsening, no precipitation occurred within the particles for times as long as 100h at these temperatures. HRTEM observations are being conducted to confirm these findings. A paper based on these results, including explanations for the absence of precipitation, is in preparation for submission to *App. Phys. Lett.* [16].

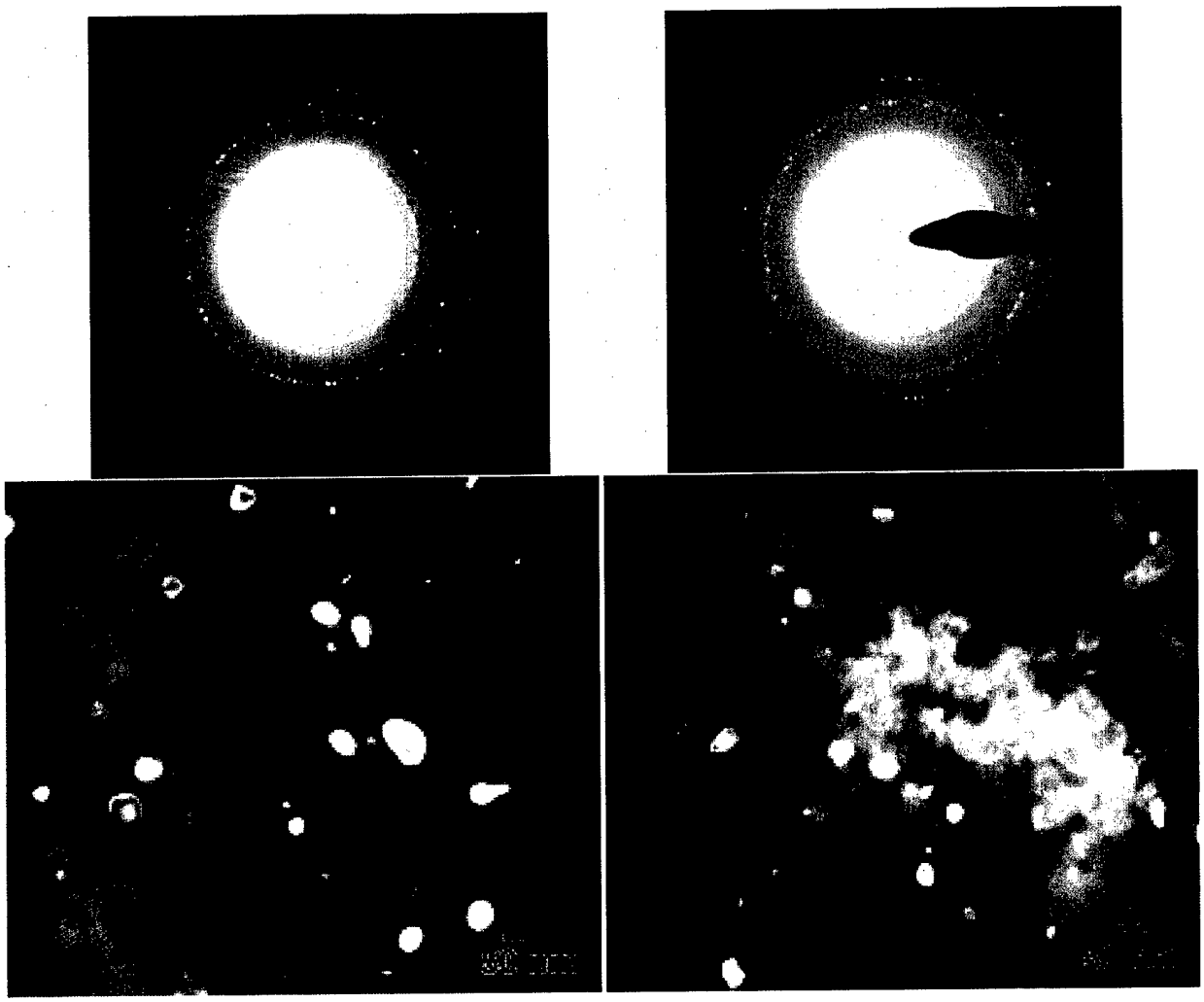

Figure 13–IGC-synthesized and then aged Al-Cu nanoparticles. (a) SAD and (b) DF micrograph from (111) reflection from particles aged at 190°C, 100h; (c) SAD pattern and (d) DF micrograph from (111) reflection from particles aged at 300°C, 100h.

3.3 Processing Bulk Structures from NanoPowders of Aluminum

The aim of this part of the project was to study the ability to consolidate nanoscale powders to bulk structures by combinations of sintering and cold/hot rolling operations and to ascertain the mechanisms of sintering and the extent to which the initial nanoscale particle size could be preserved.

For this study, pure Al nanopowders that had been produced by the exploding wire method were purchased from Argonide Inc. (Sanford, FL). The powders were cold-compacted in a stainless steel die under a pressure of 370 MPa held for 2 minutes. The effect of sintering temperature (500-650°C), sintering time (1-3h), cold rolling and hot rolling (200-400°C) on compact density, hardness and microstructure were studied. Microstructures were examined by SEM and TEM.

The as-received powders ranged in diameter from 50-150 nm, with an average around 100nm (Fig. 14). A few larger particles ranging in size from 1-5 μm were also present. Macro photographs of the compacts after various processing steps are shown in Fig. 15, and the corresponding changes in density, microhardness and microstructure are displayed in Figs. 16 and 17.

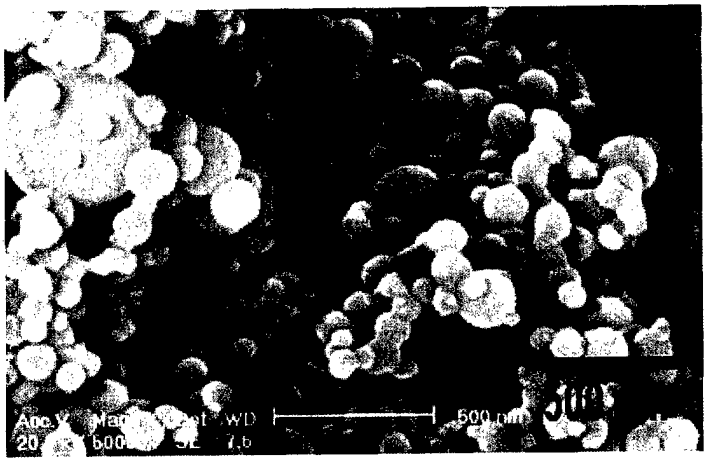

Figure 14—SEM micrograph of as-received Al nanopowders.

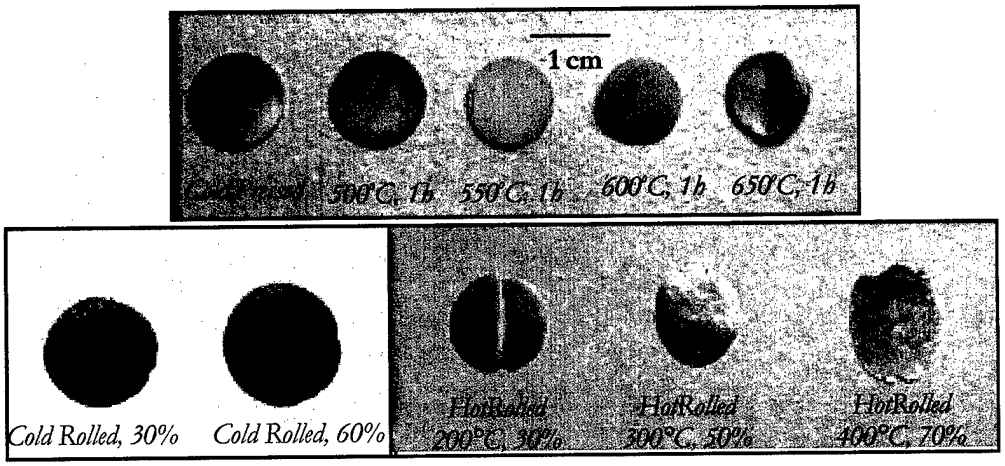

Figure 15—Macrophotographs of compacts of Al nanopowders following various indicated processing steps.

The density and hardness increased with an increase in the sintering temperature, with values approaching 97% theoretical and 100 HV, respectively, at 650°C (Fig. 16). The oxide scale present initially around the particles was intact until 500°C (Fig. 17(b), but became breached at higher sintering temperatures (600-650°C), resulting in a very interesting nanocomposite composed of Al oxide particulate in the Al matrix, Figure 17(c,d), both having nanoscale dimensions. Correspondingly, the density and hardness also increased. TEM examination (Fig. 18) revealed that the nanoscale grain size of the Al was retained after sintering, though there was also evidence for some grain growth. There was also evidence that the Al grains were deformed (i.e. changed shape) and in some cases contained twins, which is unexpected for aluminum.

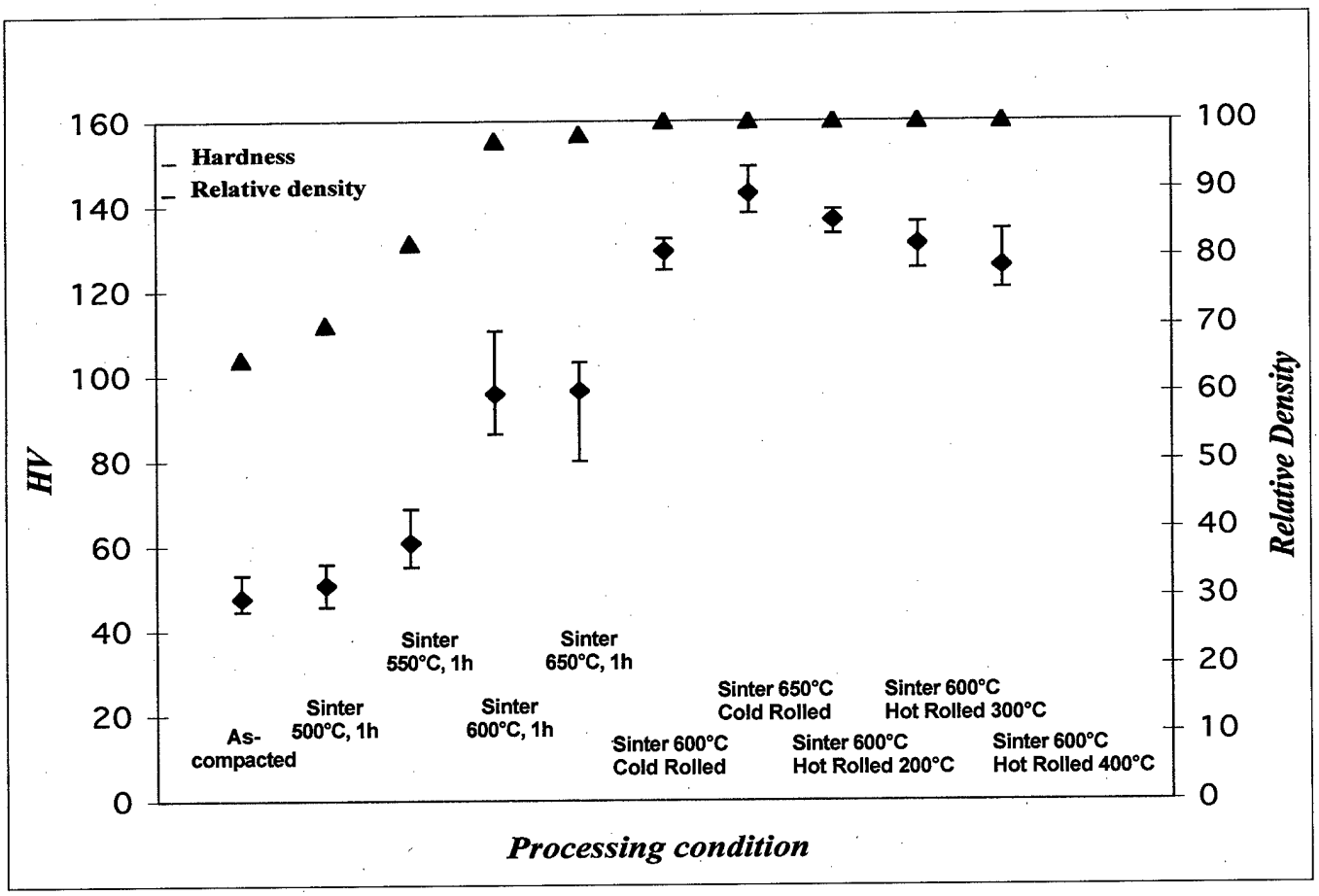

Figure 16—Changes in relative density and microhardness following various indicated processing steps.

Cold rolling was even more effective for attaining full densification (100%) and high hardness (~140 HV). The sintered compacts could be cold rolled successfully to as high as 60% reduction without macroscopic failure (Fig. 19(a)). However, examination at very high

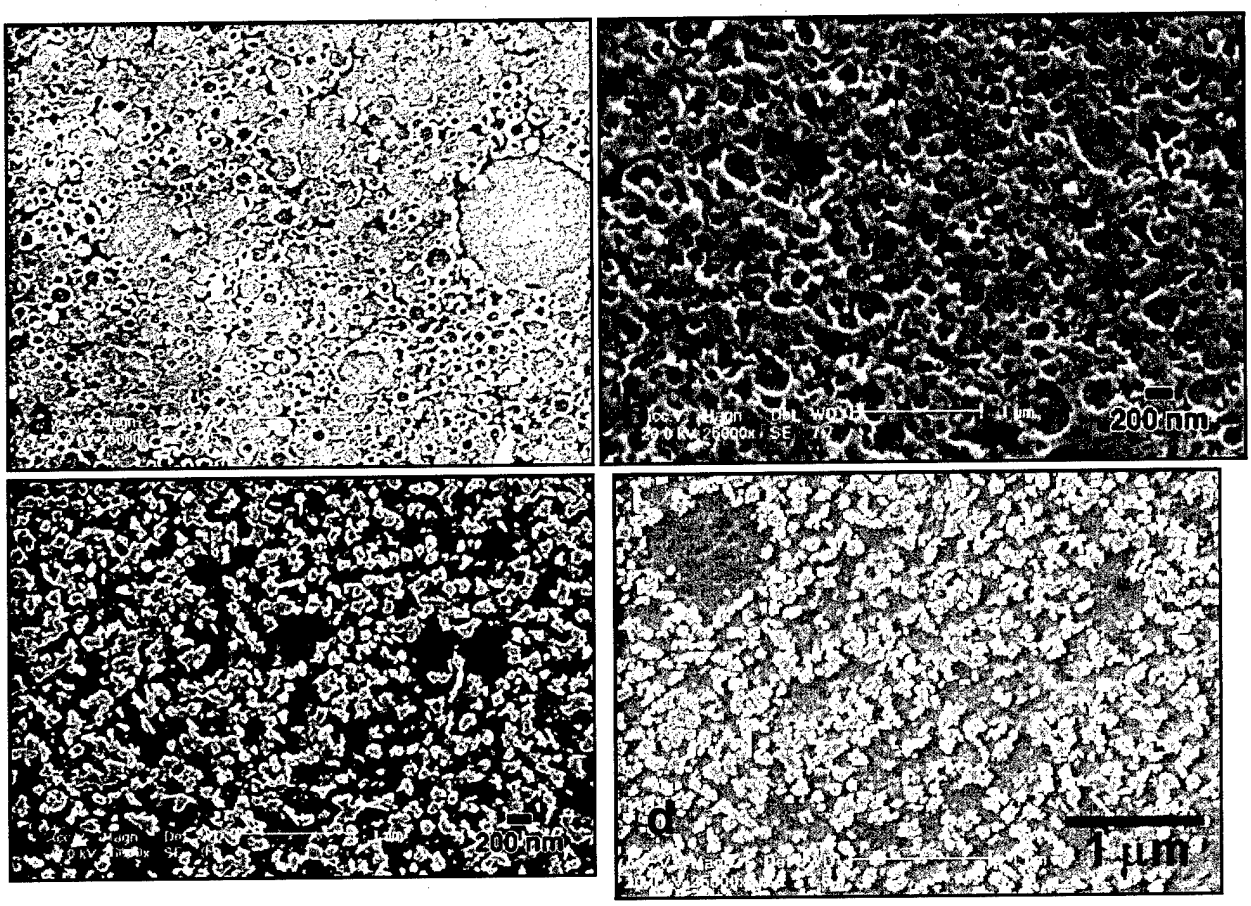

Figure 17—SEM micrographs showing microstructure of compacts of Al nanopowders following various processing steps. (a) cold-pressed; (b) cold-pressed + 500°C, 1h; (c) cold-pressed + 600°C, 1h; and (d) cold-pressed + 650°C, 1h

magnifications revealed the presence of nanoscale cracks. Hot rolling of the sintered compacts, on the other hand, led to crack-free material (Fig. 19(b), but a slight decrease in hardness, coupled with some grain growth (Fig. 20). These various results indicate that nanoscale powders can be successfully consolidated to bulk structures by thermal and thermo mechanical processing. The nanoscale dimensions of the original particles are largely retained, and simultaneously unique Al-Al oxide nanocomposites are produced with potentially attractive properties. A paper based on these results is in preparation for submission to *Metall. Mater. Trans.* [17].

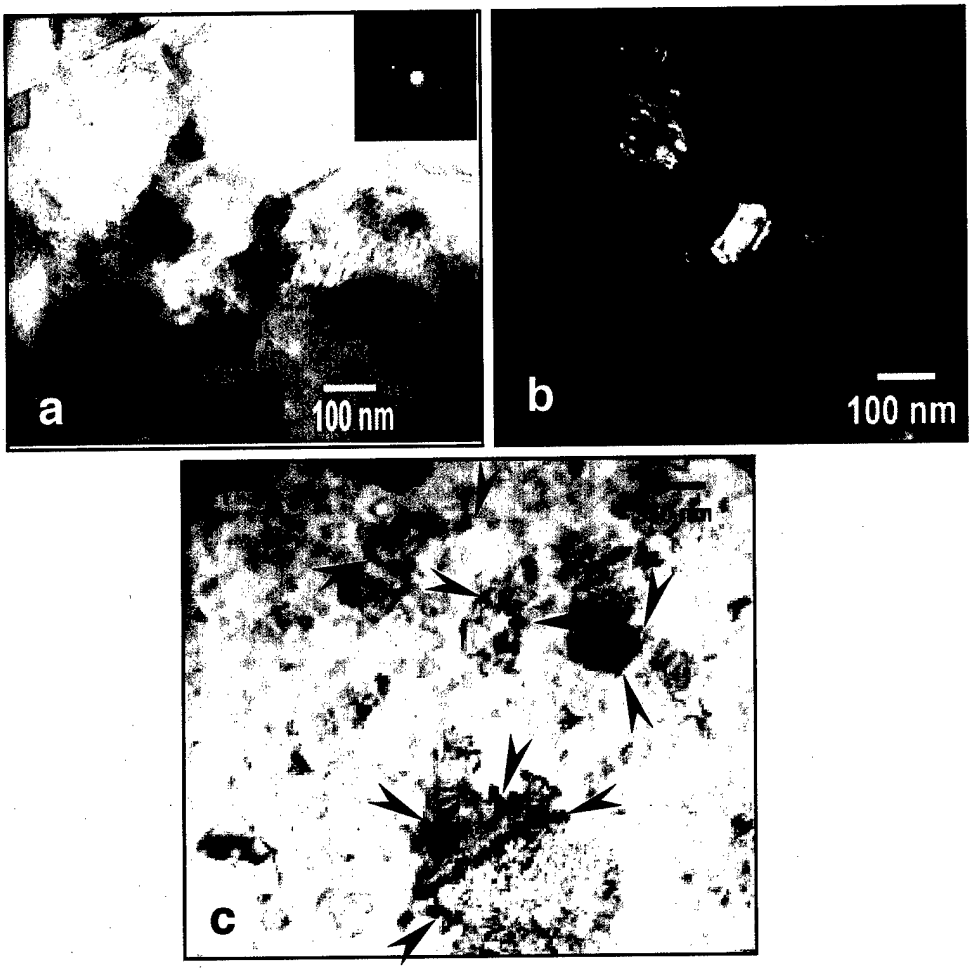

Figure 18. Al nanopowders compacted and sintered at 600°C, 1h. (a) BF TEM image; (b) DF from (111) Al reflection in inset SAD pattern showing nanoscale Al grains (evidence for grain growth present); and (c) BF micrograph showing fragmentation (arrows) of Al oxide layer into nanoscale oxide particles.

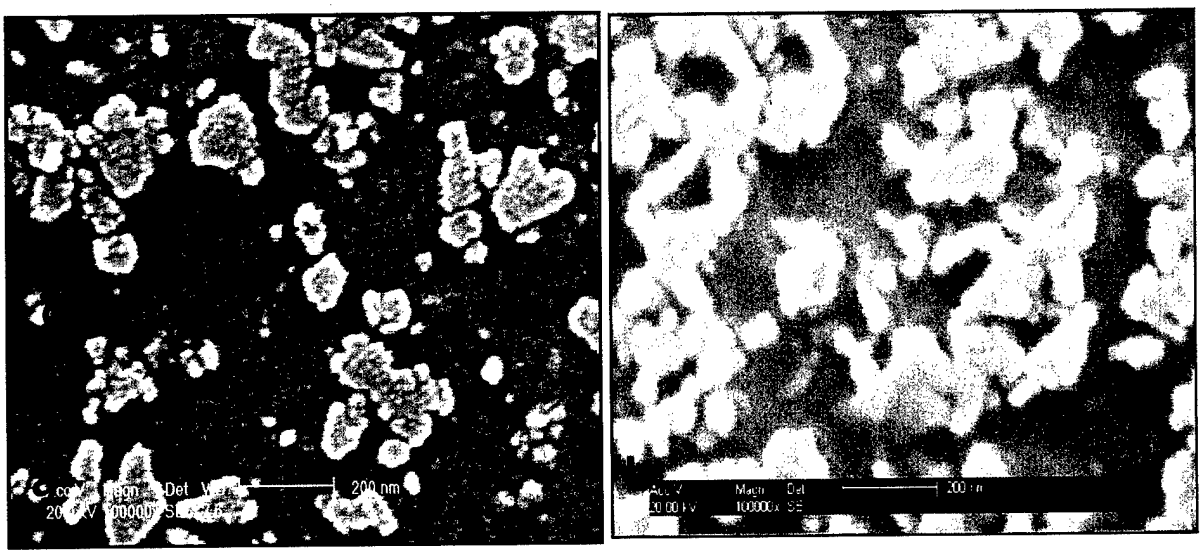

Figure 19. SEM micrographs of compacts sintered at 600°C, 1h and then (a) cold rolled 60% reduction and (b) hot rolled at 400°C, 70% reduction . Note nanocracks (encircled) in 'a' but none in 'b'.

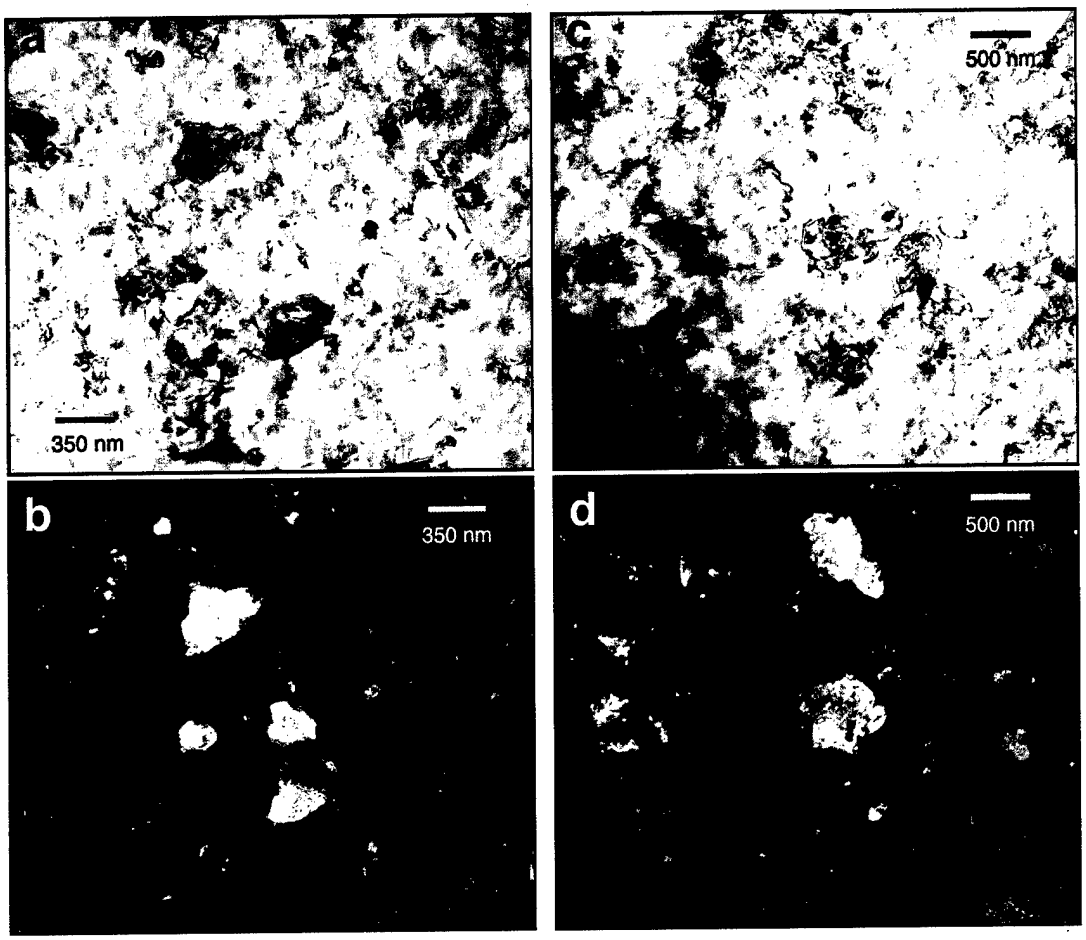

Figure 20. BF and DF TEM micrograph pairs showing microstructure of compacts sintered at 600°C, 1h and then (a,b) hot rolled 30% reduction at 200°C and (c,d) hot rolled at 400°C, 70% reduction . Note bimodal distribution of grains (0.5-1μm and 100-300 nm size).

4. PERSONNEL SUPPORTED

The personnel supported in this project include Vijay K. Vasudevan (P.I.), Jai A. Sekhar (co-PI) and graduate students Jixiong Han and Martin J. Pluth.

5. New Discoveries, Inventions or Patent Disclosures

The following are the major new findings resulting from this project.

- Nanoparticles of Al-Cu and Al-Zn were synthesized by a plasma ablation process and the transformation behavior within these particles on aging was studied.
- The particles were in the supersaturated f.c.c. state, but displayed a variation in the individual particle composition compared with the precursor ingots.
- The particles were often faceted along {111} planes and were free of dislocations; all particles were covered with a 2-4 nm Al oxide layer that protected them from further oxidation.
- During aging of the Al-Cu particles, nearly pure Cu precipitates form first along the oxide-particle interface and these transform to θ' followed by equilibrium θ-Al_2Cu.
- The structure of θ' and interface with the Al matrix were established by HRTEM.
- A spinodal structure was noted in the Al-Zn particles, which coarsened on aging into a striated f.c.c. twinned platelet structure that contained h.c.p. precipitates also in twin relation. Nearly pure h.c.p. Zn precipitates also formed along the oxide-particle interface.
- Ultra fine Al-Cu nanoparticles were synthesized by IGC; these nanoparticles were found to be quite stable against precipitation during aging.
- NanoPowders of Al could be processed via thermal and thermo mechanical means to bulk structures with high hardness and density; temperature and time of sintering have a dominant effect.
- The sintering process led to breakup of the oxide scale, leading to an interesting nanocomposite composed of 100-200 nm amorphous Al oxide dispersed in a bimodal nanometer-micrometer size Al matrix grain matrix. Ultra fine (10-20 nm size) Al oxide particles were also present and effectively pinned the grain boundaries.
- The sintered compacts could be successfully cold and hot rolled to high reductions in multiple passes, and these procedures gave full densification and high hardness. Nanocracks were observed in the cold rolled materials, but were absent in the hot rolled materials.

6. TRANSITIONS/INTERACTIONS

The nanoparticles studied herein were synthesized by Nanotechnologies, Inc., Austin, TX. In addition, ultra fine nanoparticles of Al-Cu alloys were synthesized with the help of Dr. Jeff Eastman and his IGC equipment at ANL. Meetings have been held with scientists at AFRL (Drs. D. Dimiduk, D. Miracle and K. Williams) to discuss the project goals and results. Part of the electron microscopy work was performed using the facilities available at the Air Force Research Laboratory, Materials Directorate, WPAFB, Dayton, OH; the Argonne National Laboratory, Electron Microscopy Center, Argonne, IL; and the National Institute of Materials Science, Nanomaterials Laboratory (Dr. Kazuo Furuya), Tsukuba, Japan. The project results have also been disseminated through publications (1 published, 1 close to submission and 2 under preparation) and through invited and contributed talks at universities, national/international technical conferences and at the annual AFOSR Metallic Structural Materials Workshop.

7. REFERENCES CITED

1. M. C. Roco, R. S. Williams and P. Alivisatos (eds.), "Nanotechnology Research Directions, IWGN Workshop Report: Vision for Nanotechnology R&D in the Next Decade," on behalf of *National Science and Technology Council /Interagency Working Group on Nanotechnology, Intern. Technology Research Institute, World Technology Division*, Loyola College (1999).

2. R. W. Siegel, E. Hu and M. C. Roco (eds.), "Nanotechnology Research Directions, IWGN Workshop Report: Nanostructure Science and Technology," on behalf of *National Science and Technology Council /Interagency Working Group on Nanotechnology, Intern. Technology Research Institute, World Technology Division*, Loyola College (1999).

3. H. Gleiter, "Nanocrystalline Materials," *Progr. Mater. Sci.*, **33**, 223-315 (1989).

4. R. Uyeda, "Studies of Ultrafine Particles in Japan: Crystallography, Methods of Preparation and Technological Applications," *Progr. Mater. Sci.*, **35**, 1-96 (1991).

5. R. P. Andres et al., "Research Opportunities on Clusters and Cluster-Assembled Materials—A Department of Energy, Council on Materials Science Panel Report," *J. Mater. Res.*, **4**, 704-736 (1989).

6. J. A. Eastman, L. J. Thompson and D. J. Marshall, *Nanostr. Mater.*, **2**, 377 (1993).

7. M. N. Rittner, J. A. Eastman and J. R. Weertman, Synthesis and Properties Studies of Nanocrystalline Al-Al_3Zr," *Scripta Metall. Mater.*, **7**, 841-846 (1994).

8. M. N. Rittner, J. R. Weertman and J. A. Eastman, "Structure-Property Correlations in Nanocrystalline Al-Zr Alloy Composites," *Acta Mater.*, **44**, 1271-1286 (1996).

9. P. G. Sanders, J. A. Eastman and J. R. Weertman, "Elastic and Tensile Behavior of Nanocrystalline Copper and Palladium," *Acta Mater.*, **45**, pp. 4019-4025 (1997).

10. X. K. Sun, H. T. Cong, M. Sun and Y. C. Yang, "Preparation and Mechancial Properties of Highly Densified Nanocrystalline Al," *Metall. Mater. Trans.*, **31A**, pp. 1017-1024 (2000).

11. C. C. Koch, "Bulk Behavior of Nanostructured Materials," in ref. [2], pp. 93-109 (1999).

12. H. Kung and T. C. Lowe, "Superstrong Materials by Nanostructuring," in Ref. [1], pp. 13-14 (1999).

13. M. Shinn, L. Hultman and S. A. Barnett, "Growth, Structure, and Microhardness of Epitaxial TiN/NbN Superlattices, *J. Mater. Res.*, **7**, pp. 901-911 (1992).

14. V. K. Vasudevan and J. A. Sekhar, "Transformation Behavior in Nanoscale Binary Aluminum Alloys," in: *Advances in the Metallurgy of Aluminum Alloys*, TMS, Warrendale, PA, pp. 398-405 (2001).

15. J. Han, M. J. Pluth, K. Furuya, J. A. Sekhar and V. K. Vasudevan, "Transformation Behavior in Nanoscale Powders of a Binary Al-Cu and Al-Zn Alloys," *Acta Mater.*, close to submission.

16. J. Han, J. A. Sekhar, J. A. Eastman and V. K. Vasudevan, "Synthesis of Al-Cu Nanoparticles by Inert Gas Condensation and Their Aging Behavior," *Appl. Phys. Lett.*, in preparation.

17. M. J. Pluth, J. Han, J. A. Sekhar and V. K. Vasudevan, "Processing Bulk Structures From Nanopowders of Aluminum, *Metall. Mater. Trans.*, in preparation.

18. J. M. Silcock, T. J. Heal and H. K. Hardy, *J. Inst. Metals*, **82**, 239-248 (1953-54).

19. L. F. Mondolfo, *Aluminum Alloys, Structure and Properties*, Butterworths USA, p. 254 (1976).

20. V. Gerold and W. Merz, *Scripta Metall.*, **1**, 33 (1967)

21. K.. Rundman and J. E. Hilliard, *Acta Metall.*, **15**,1025 (1967).

22. J. E. Hilliard, "Spinodal Decomposition," *in: Phase Transformations*, American Society for Metals, Metals Park, OH, 497(1970).

8. PUBLICATIONS

1. V. K. Vasudevan and J. A. Sekhar, "Transformation Behavior in Nanoscale Binary Aluminum Alloys," in: *Advances in the Metallurgy of Aluminum Alloys*, TMS, Warrendale, PA, pp. 398-405 (2001).

2. J. Han, M. J. Pluth, K. Furuya, J. A. Sekhar and V. K. Vasudevan, "Transformation Behavior in Nanoscale Powders of Binary Al-Cu and Al-Zn Alloys," *Acta Mater.*, close to submission.

3. J. Han, J. A. Sekhar, J. A. Eastman and V. K. Vasudevan, "Synthesis of Al-Cu Nanoparticles bInert Gas Condensation and Their Aging Behavior," *Appl. Phys. Lett.*, in preparation.

4. M. J. Pluth, J. Han, J. A. Sekhar and V. K. Vasudevan, "Processing Bulk Structures From Nanopowders of Aluminum, *Metall. Mater. Trans.*, in preparation.

9. PRESENTATIONS

Invited

1. "Processing Bulk Structures from Nanopowders of Aluminum," in: *Symposium on Suaces and Interfaces in Nanostructured Materials*, TMS Annual Meeting, Charlotte, NC, March 15-17 (2004).

2. "Phase Transformations in Nanoscale Aluminum Alloys," *Department of Mechanical, Materials and Aerospace Engineering, Illinois Institute of Technology*, Chicago, IL, August 29 (2003).

3. "Transformation Behavior in Nanoscale Aluminum Alloys," in: *International Conference on Materials for Advanced Technologies, Symposium on Science and Technology of Nanomaterials,*, Materials Research Society, Singapore, Dec 7-11 (2003).

4. "Lightweight, High-Strength, Age-Hardenable Nanoscale Materials," *AFOSR Metallic Materials Contractor's Meeting,* Bar Harbor, ME, Aug. 12-14 (2002).

5. "Lightweight, High-Strength, Age-Hardenable Nanoscale Materials," *AFOSR Metallic Materials Contractor's Meeting,* Snowbird, UT, Aug. 19-21 (2001).

Contributed

6. J. Han, M. J. Pluth, K. Furuya, J. A. Sekhar and V. K. Vasudevan, "Transformation Behavior in Nanoscale Powders of Binary Al-Cu and Al-Zn Alloys," *in Symposium on Surfaces and Interfaces in Nanostructured Materials*, TMS Annual Meeting, Charlotte, NC, March 15-17 (2004).

7. M. J. Pluth, J. A. Sekhar and V. K. Vasudevan, "Transformation Behavior in Nanoscale Powders of a Binary Al-Zn Alloy," *in: International Conference on Nanostructured Materials*, TMS/MST '03 Fall Meeting, Chicago, IL, November 7-11 (2003).

8. J. Han, K. Furuya, J. A. Sekhar and V. K. Vasudevan, "Transformation Behavior in Nanoscale Powders of a Binary Al-Cu Alloy," *in: International Conference on Nanostructured Materials*, TMS/MST '03 Fall Meeting, Chicago, IL, November 7-11 (2003).

9. M. J. Pluth, J. Han, J. A. Sekhar and V. K. Vasudevan, "Processing Bulk Structures from Nanoscale Powders of Al," *in: International Conference on Nanostructured Materials*, TMS/MST '03 Fall Meeting, Chicago, IL, November 7-11 (2003).

10. J. Han, K. Furuya, J. A. Sekhar and V. K. Vasudevan, "Transformation Behavior in Nanoscale Powders of a Binary Al-Cu Alloy," *in:: International Conference on Structures and Properties of Nanocrystalline Materials*, TMS Annual Meeting, San Diego, CA, March 2-6 (2003).

11. M. J. Pluth, J. A. Sekhar and V. K. Vasudevan, "Transformation Behavior in Nanoscale Powders of a Binary Al-Zn Alloy," *in: International Conference on Structures and Properties of Nanocrystalline Materials*, TMS Annual Meeting, San Diego, CA, March 2-6 (2003).

12. M. J. Pluth, J. Han, J. A. Sekhar and V. K. Vasudevan, "Processing Bulk Structures from Nanoscale Powders of Al," *in: International Conference on Structures and Properties of Nanocrystalline Materials*, TMS Annual Meeting, San Diego, CA, March 2-6 (2003).

13. J. Han, M. J. Pluth, J. A. Sekhar and V. K. Vasudevan, "Transformation Behavior in Nanoscale Binary Aluminum Alloy Powders," *in: International Conference on Nanostructured Materials*, Orlando, FL, June (2002).

14. M. J. Pluth, J. Han, J. A. Sekhar and V. K. Vasudevan, "Transformation Behavior in Nanoscale Binary Aluminum Alloys," *in: International Conference on Ultrafine-grained Materials,* TMS Annual Meeting, Seattle, WA, Feb. (2002).

15. J. Han, M. J. Pluth, J. A. Sekhar and V. K. Vasudevan, "Transformation Behavior in Nanoscale Binary Aluminum Alloys," *in: International Conference in Advanced Materials and Processes*, Indian Institute of Technology, Kharagpur, India, Feb. (2002).

16. J. Han, M. J. Pluth, J. A. Sekhar and V. K. Vasudevan, "Transformation Behavior in Nanoscale Binary Aluminum Alloys," *in: Staley Symposium on Aluminum Alloys*, ASMI Fall meeting, Indianapolis, IN, October (2001).

10. ACKNOWLEDGEMENTS/DISCLAIMER

Financial support for this work from the Air Force Office of Scientific Research, USAF, under grant no. F49620-01-1-0127 and Dr. Craig Hartley, Program Monitor, is deeply appreciated. The views and conclusions contained herein are those of the authors and should not be interpreted as necessarily representing the official policies or endorsements, either expressed or implied, of the AFOSR or the U.S. Government. The help provided by Nanotechnologies, Inc., Austin, TX (Dr. Dennis Wilson) in synthesizing the Al-Cu and Al-Zn nanoparticles; MHI, Inc., Cincinnati, OH (Dr. G. S. Reddy) for making the alloy ingots; and Argonne National Laboratory, MSD Argonne, IL (Dr. Jeff Eastman) for use of the IGC facilities to synthesize the ultra fine Al-Cu nanoparticles is gratefully acknowledged. The authors also thanks the Air Force Research Laboratory, Materials Directorate, WPAFB, Dayton, OH; the Argonne National Laboratory, Electron Microscopy Center, Argonne, IL; and the National Institute of Materials Science, Nanomaterials Laboratory (Dr. Kazuo Furuya), Tsukuba, Japan for providing the use of the high resolution electron microscopy and nanoprobe EDS facilities in the characterization work.